Available online at www.sciencedirect.com
ScienceDirect
Computers and Mathematics with Applications 55 (2008) 1842–1853
An International Journal
computers & mathematics
with applications
www.elsevier.com/locate/camwa

# Synchronization among tumour-like cell aggregations coupled by quorum sensing: A theoretical study

J.C. Misra*, A. Mitra

*Centre for Theoretical Studies/Department of Mathematics, Indian Institute of Technology, Kharagpur - 721302, India*

Received 23 May 2007; accepted 7 June 2007

**Abstract**

In this paper we examine the synchronization of a collection of repressilators in tumour-like cell aggregations coupled using quorum sensing. The force of diffusion that exists between neighbouring cells on the surface of the tumour has been paid due consideration. The study reveals that such a coupled system would show synchronization. Our computational results further show that such a prediction holds not only for individual tumours but also for multiple tumours coupled together. The degree of synchronization is found to be dependent on the strength of coupling, which is in turn determined by the cell density.


*Keywords:* Repressilator; Synchronization; Quorum sensing; Cell aggregation; Genetic oscillators

## 1. Introduction

Medical researchers today are quite concerned about different issues related to the synchronization of biological oscillators and the mechanisms by which this is achieved. The said phenomenon is of utmost importance in many physiological conditions. For instance, the human heart functions via alternate contractions and relaxations of its chambers, the auricles and the ventricles, set off by signals from the sino-atrial node, also known as the pacemaker. This tissue consists of a collection of myocytes that synchronously generate electrical impulses to trigger the contractions of the heart. However, several important questions regarding synchronization are yet to be explored.

Of grave concern in health sciences today is the manifestation of the deadly disease cancer, and its treatment modalities. Sometimes the occurrence of tumours can lead to carcinogenesis. Analytical studies of tumours can be broadly classified into three parts based on the particular stage in the life cycle of a tumour they examine: *avascular tumour growth*, *tumour-induced angiogenesis* and *metastasis*. The first approach models the incipient stages of the tumour that results in a benign growth. The tumour is localized and sufficiently small. The latter two approaches model the malignant stages of the tumour when the tumour obtains its own blood supply (angiogenesis) and can use it to be transported to different parts of the body (metastasis). While these approaches are more relevant to cancer cure, they entail a prohibitively complex model without sufficient experimental data for verification.

One cannot ignore the importance of such a study, although it involves a large amount of complexities. Indeed any theoretical approach requires experimental data in order to quantify its predictions. However, we can make educated

* Corresponding author.
*E-mail address:* jcm@maths.iitkgp.ernet.in (J.C. Misra).

0898-1221/$ - see front matter 
doi:10.1016/j.camwa.2007.06.027

guesses regarding the situations that are likely to appear *in vivo* before proceeding towards experimental analysis — a feasible approach in many cases where a direct experiment can be difficult or even impossible. Investigations on tumours fall into such a category. We are unable to simulate, with a significant degree of authenticity, the cellular conditions under which a tumour initiates and propagates in the human body. In the present day and age, one cannot conduct clinical trials on human subjects in order to verify the accuracy of the predictions made. Moreover, experimental data obtained from tests on sub-human primates are not directly applicable to humans. This necessitates the modelling of theoretical constructs that approximate the changes taking place at a microscopic level inside human tissue.

Biological oscillators are quite common in nature. They are extremely wide in their scope, occurring in several phenomena such as circadian rhythms and in specialized systems like the endocrine system. Organisms are continuously subjected to dynamic changes enforced by the external environment and also by the cyclic behaviour induced by internal cellular clocks. Instances of the latter include the cardiac pacemaker which is found at the sino-atrial node in the human heart and the suprachiasmatic nuclei (SCN) located in the human hypothalamus that is responsible for endogenous 'circadian rhythms'. These oscillators are specialized structures composed of thousands of inherently diverse clock cells that still manage to oscillate in unison. The mechanism behind such collective behaviour remains as one of the nature's abiding mysteries.

Clock cells operate via biochemical networks that consist of numerous intertwined regulatory feedback loops. The sheer complexity of these networks serves as a deterrent for the understanding of underlying mechanisms behind their function. Synthetic genetic networks bypass this problem, doing away with the overwhelming complexity of such systems while maintaining certain levels of control that enable us to examine their functions in detail. The synthetic biological oscillator, called the "repressilator", was developed in *Escherichia coli* with this very purpose in mind. It consists of a network of three transcriptional genes that inhibit each other in a cyclic manner. Individual cells in the culture were found to oscillate spontaneously.

As a logical step forward, a mode of inter-cell coupling was introduced that would improve the oscillatory response in a systemic manner. Quorum sensing as a means for population control and synchronization has been studied in recent times. Hahnfeldt et al. [1] gave a dynamical theory to explain the growth, treatment response and postvascular dormancy of tumour. In a recent communication, McMillen et al. [2] have demonstrated theoretically that a population of identical genetic oscillators can be synchronized using quorum sensing. Garcia-Ojalvo et al. [3] have also shown quorum sensing as a means to induce synchronization in an array of noisy coupled repressilators. Several attempts to model the tumour growth have been made in recent years by different researchers [4–7].

For the purpose of our study, we will use cells that are structurally identical to those used in [3].

The present investigation is primarily based on the introduction of cellular aggregations into the said problem. While in the studies referred to above, the researchers had considered single cells in solution coupled by quorum sensing, we develop here a new mathematical model, incorporating the level of complexities that arise due to the coupling of each cell to its neighbours via diffusion. Such a situation is prevalent in a 'tumour-like' mass that consists of several layers of cells. However, in such a structure only the outermost layer of cells are in direct contact with the external solution and hence only these are coupled by quorum sensing.

The continuum hypothesis of tumour structure assumes that there is an absence of well-defined layers in a tumour. There is a gradual drop in cell density from the surface of the tumour to the interior. We adopt this hypothesis in our study. Moreover, Ward and King [4] have modelled avascular tumour growth and found that the live cell density falls quite sharply from the outer surface of the tumour to the interior. Hence, it is reasonable to assume that the outermost layer is the only one where we find live cells. Besides, on the surface of a tumour a cell can be in physical contact, and hence capable of exchanging products via diffusion, with several cells. In our model, we have incorporated such an exchange between a cell and two of its neighbours.

In the following sections, we have first examined the case of a single cell aggregation (which for our purposes we call a 'tumour') in isolation. We consider a single tumour and check whether its own cells synchronize under quorum sensing. Subsequently we move on to a population of 'tumours' coupled by quorum sensing and find that they synchronize globally when we increase the strength of the coupling.

## 2. The proposed model

The repressilator consists of three genes combined together in a pathway. The products of each inhibit the transcription of the others in a cyclic manner [3]. The relationship is shown in the diagram (see Fig. 2.1). The gene lacI

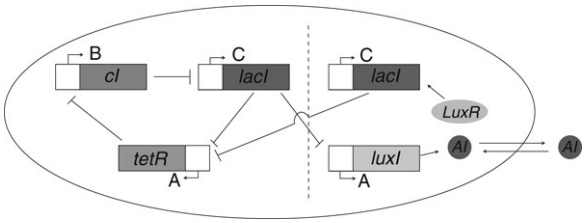


Fig. 2.1. Scheme of the repressilator network coupled to a quorum sensing mechanism [3]. The original repressilator module is located at the left of the vertical dashed line, and the new coupling module appears at the right. The letters A, B and C correspond to the notations used in the text.

(origin: *E. coli*) produces the protein LacI, which inhibits the production of the protein TetR, by the gene tetR (from the tetracycline resistant transposon Tn10). The protein TetR, in turn, inhibits the transcription of the gene cI (from λ phage). The product of the latter, CI, inhibits the production of LacI, hence completing the cycle. A modular addition to the design was also proposed for the purpose of coupling a population of cells with the above network as a part of their internal machinery. The quorum sensing mechanism of the bacterium *Vibrio fischeri*, provides the perfect means of achieving the requisite means of coupling. *V. fischeri* exists in symbiotic association with certain marine hosts as a part of specialized light-producing structures. The intra-cellular communication occurs via two proteins, the first one of which, LuxI, produces a molecule known as auto-inducer (AI), which permeates the cell membrane freely owing to its small size. The second protein, LuxR, binds with the AI molecule to form a complex that activates transcription of various genes, including some that code for light-producing enzymes.

This inter-cell signalling apparatus has been incorporated into the repressilator by placing the gene that encodes LuxI under the control of the repressilator protein LacI (cf. Fig. 2.1). Additionally, a second copy of another repressilator gene (such as lacI) is inserted into the *E. coli* cell such that the complex LuxR-AI induces its expression. As a result a feedback loop appears in the repressilator, which is reinforced by similar levels of LacI among neighbouring cells.

To model the dynamics of gene expression in the cells, one has to keep track of the evolution of all mRNAs and protein concentrations from every cell in the network. The dynamics of the system described above can be represented by the following set of differential equations

$$\begin{aligned}
\frac{\mathrm{d}a_i}{\mathrm{d}t} &= -a_i + \frac{\alpha}{1 + C_i^n} \\
\frac{\mathrm{d}b_i}{\mathrm{d}t} &= -b_i + \frac{\alpha}{1 + A_i^n} \\
\frac{\mathrm{d}c_i}{\mathrm{d}t} &= -c_i + \frac{\alpha}{1 + B_i^n} + \frac{\kappa S_i}{1 + S_i}.
\end{aligned} \tag{2.1}$$

Here $a_i$, $b_i$ and $c_i$ are the concentrations in cell $i$ of mRNA produced by the genes tetR, cI and lacI respectively, and the respective protein concentrations are represented by $A_i$, $B_i$ and $C_i$. The two copies of the lacI gene are assumed to be identical. $S_i$ denotes the concentration of the auto-inducer molecule inside each cell. The Hill coefficient $n$ takes care of the effect of co-operativity in the repression mechanisms, whereas the activation of the AI molecule follows standard Michaelis–Menten kinetics. The model is made dimensionless in the same way as in [3]. The protein levels are measured in terms of their Michaelis constants, i.e. the concentration at which their transcription rate is half of its maximum. The concentration of the auto-inducer, denoted by $S_i$, is also scaled by its Michaelis constant. $\alpha$ is the dimensionless rate of transcription, and $\kappa$ is the maximal increase in the transcription of lacI in the presence of large amounts of AI.

The protein dynamics is given by:

$$\frac{\mathrm{d}A_i}{\mathrm{d}t} = \beta(a_i - A_i) \tag{2.2}$$

and similarly for $B_i$ (and $b_i$) and $C_i$ (and $c_i$). The parameter $\beta$ is the ratio between the mRNA and protein lifetimes.

Finally the intra-cellular production of the auto-inducer is controlled by the degradation and synthesis (within the cell), diffusion into and from the neighbouring cells in the tumour and diffusive exchange with the external environment. If we assume the lifetimes of the TetR and LuxI proteins to be equal, their dynamics are also same, and hence can be expressed by the same variable in the computer simulations of the model. We also assume that only the cells on the surface of the tumour, contribute to the external concentration of the AI. These cells are, in turn, coupled with each other via diffusion through their cell membranes. The diffusion of the small AI molecule is governed by the Fick's law and hence is assumed to be inversely proportional to the thickness of the membrane across which the diffusion takes place. Hence the evolution of the auto-inducer is given by

$$\frac{\mathrm{d}S_i}{\mathrm{d}t} = -k_{s0}S_i + k_{s1}A_i - \eta(S_i - S_e) - \eta_d(2S_i - S_{i-1} - S_{i+1}) \tag{2.3}$$

where $\eta$ is the constant of diffusion governing the transfer of AI across the cell membrane and $\eta_d$ is the constant governing the diffusion between neighbouring cells. We assume $\eta_d$ to be equal to $\eta/2$ according to the Fick's law of diffusion as described above. The parameters $k_{s0}$, $k_{s1}$, $\eta$ & $\eta_d$ have been rendered dimensionless. $S_e$ represents the concentration of AI in the external environment and its dynamics are given by

$$\begin{aligned}\frac{\mathrm{d}S_e}{\mathrm{d}t} &= -k_{se}S_e + \eta_{\mathrm{ext}}\sum_{j=1}^{N}(S_j - S_e)\\ &\equiv -k_{se}S_e + k_{\mathrm{diff}}(\overline{S} - S_e)\end{aligned} \tag{2.4}$$

where $\eta_{\mathrm{ext}}$ is the constant of diffusion governing the transfer of AI from the cell to the external environment and $\overline{\ldots}$ indicates the average over all the cells. The diffusion rate is given by $k_{\mathrm{diff}} = \eta_{\mathrm{ext}}N$ and the degradation rate is given by $k_{se}$.

The modelling approach described above assumes a uniform cell density as opposed to the situations where we have cell growth (where density is reduced) and cell division (where density is increased). These are usual approximations in this kind of study and replicate, quite accurately, the situation encountered in a well-controlled chemostat. We first assume that all the cells in the above equations are on the surface of the same tumour. Subsequently the model is extended to the case of multiple tumours in which we will have $k$ replicates of the Eqs. (2.1)–(2.4). In the latter case, $N$ (in Eq. (2.4)) is replaced by $kN$, with $N$ representing the number of cells in each tumour.

### 2.1. The quasi-steady-state approximation

To facilitate our work, we make the quasi-steady-state approximation, i.e. the instantaneous rate of change in the external concentration of AI ($\mathrm{d}S_e/\mathrm{d}t$) is assumed to be zero. Hence, the extra-cellular concentration of the auto-inducer can be represented by:

$$S_e = \frac{k_{\mathrm{diff}}}{k_{se} + k_{\mathrm{diff}}}\overline{S} \equiv Q\overline{S}. \tag{2.5}$$

We note that $Q$ is dependent on the cell density $\frac{\delta N}{V_{\mathrm{ext}}}$ as

$$k_{\mathrm{diff}} = \eta_{\mathrm{ext}}N = \frac{\delta N}{V_{\mathrm{ext}}}$$

where $V_{\mathrm{ext}}$ is the total extra-cellular volume, and hence,

$$Q = \frac{k_{\mathrm{diff}}}{k_{se} + k_{\mathrm{diff}}} = \frac{\delta N/V_{\mathrm{ext}}}{k_{se} + \delta N/V_{\mathrm{ext}}}.$$

This shows that $Q$ is linearly proportional to cell density $\delta N/V_{\mathrm{ext}}$ if it is much smaller than the external degradation rate, $k_{se}$. We will now examine the dynamics of the above system as predicted by our numerical simulations.

## 3. Numerical results

The numerical simulations of the proposed model yield encouraging results. We conduct the simulations in two parts:

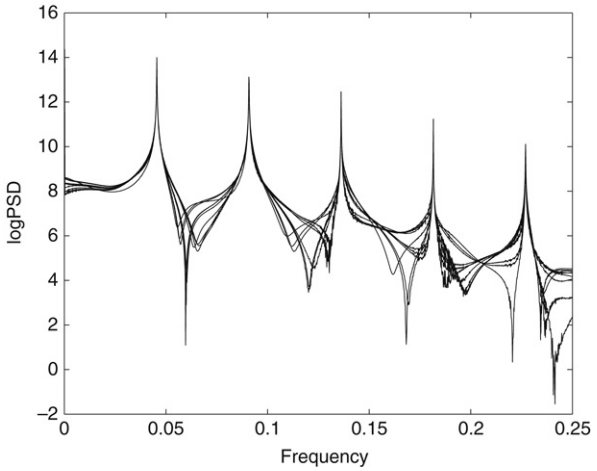


Fig. 3.1. Power Spectra of 10 cells superposed to demonstrate synchronization when $Q = 0.6$ and $N = 1000$.

1. Single Tumour Case
2. Multiple Tumour Case.

In the first case we carry out simulations for a single tumour in isolation, with the cells on its surface coupled by quorum sensing. In the second case we extend the system to multiple tumours all oscillating independently, and also coupled by quorum sensing. The simulations are conducted on an AMD-Athlon PC with programs written using ANSI C and Matlab 6.5. The values of the various parameters used for the above are as follows: $\alpha = 216$, $\kappa = 20$, $\eta = 2$, $n = 2$, $k_{s0} = 1$, $k_{s1} = 0.01$. We use the Gaussian distribution of Matlab to generate the lifetime ratios, $\beta$, for the cells.

### *3.1. Single tumour case*

We start our simulations with a single tumour having $N = 100$ cells on its surface coupled by quorum sensing. All the cells start with the same initial conditions. The lifetime ratios ($\beta$) of the cells are chosen randomly from a Gaussian distribution with $\mu = 1$ and $\sigma = 0.05$ in order to introduce a controllable variability. We then conduct simulations with different values of cell density $Q$ to denote different levels of coupling. We also perform the simulation with $N = 1000$ cells.

For both the above cases, i.e., for $N = 100$ and $N = 1000$, when we have $Q = 0.2$, we find a large spread of frequencies between 0.4 and 0.45 among the cells. This indicates little or no synchronization. However, when we increase the strength of coupling, i.e., increase the value of $Q$ from 0.2 gradually to 0.6 there is a marked improvement in the coherence of the individual cells. In spite of having several different values of $\beta$, the cells synchronize almost immediately with high $Q$. In fact for $Q = 0.6$ we have almost complete synchronization (see Figs. 3.2 and 3.3).

An alternative approach to verify the synchronization that takes place would be to examine the power spectrum of the time series data in order to determine the frequencies of each of the cells involved. The first peak on the power spectrum indicates the fundamental frequency of oscillation of the cell. We plot the power spectra of 10 cells (see Fig. 3.1), and observe that the first peak for each, coincides.

The above results indicate that the individual cells in a tumour, when coupled via the twin forces of quorum sensing and diffusion to and from neighbouring cells, synchronize to a single frequency. The degree of synchronization depends on the strength of coupling, or in other words, the value of $Q$. The next step in our analysis is to extend the above system to multiple tumours and examine the local and global synchronization for varying degrees of coupling.

### *3.2. Multiple tumour case*

We first consider the case where the number of tumours, $k$, is 10 with $N = 100$ actively diffusing cells in each. The individual behaviour of the tumours is the same as in the single tumour case. This is perhaps not surprising as the

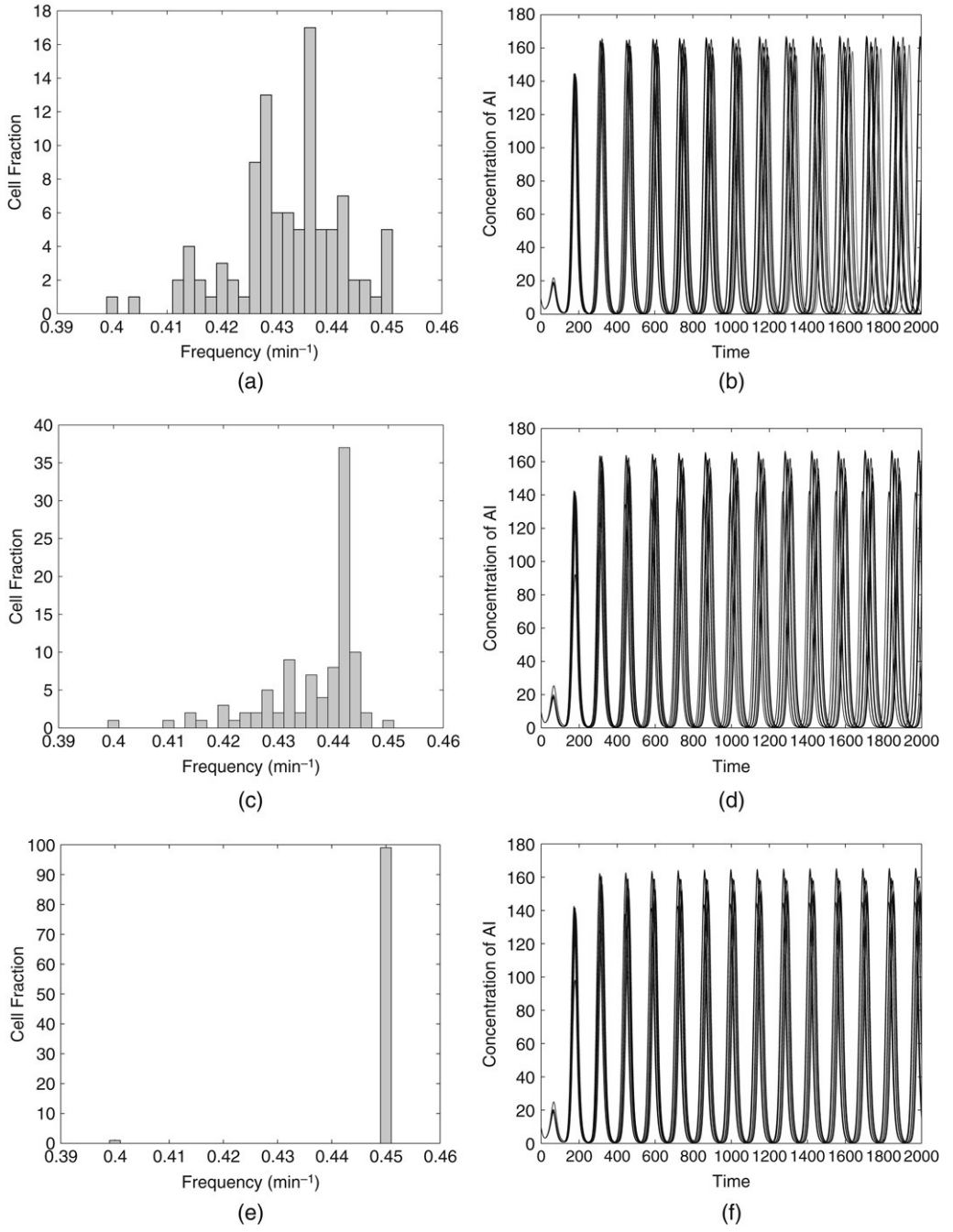


Fig. 3.2. Frequency histograms and time series plots for (a) & (b) $Q = 0.2$, (c) & (d) $Q = 0.4$ and (e) & (f) $Q = 0.6$, for the single tumour case when $N = 100$.

conditions for a particular tumour are almost identical as when we consider one tumour in isolation. This behaviour does not change even when we increase the number of tumours in the system to 100 (cf. Fig. 3.5).

This shows that even in a system with several tumours having independently oscillating cells, synchronization takes place individually within each tumour on coupling instead of a simply global synchrony that earlier results seem to indicate. The degree of synchronization is shown to be dependent on the strength of coupling.

Thus the major point of interest to us is whether there is also a global synchronization in our system. In order to examine this possibility we plot global frequency histograms for different values of $Q$ for the two cases when $k = 10$

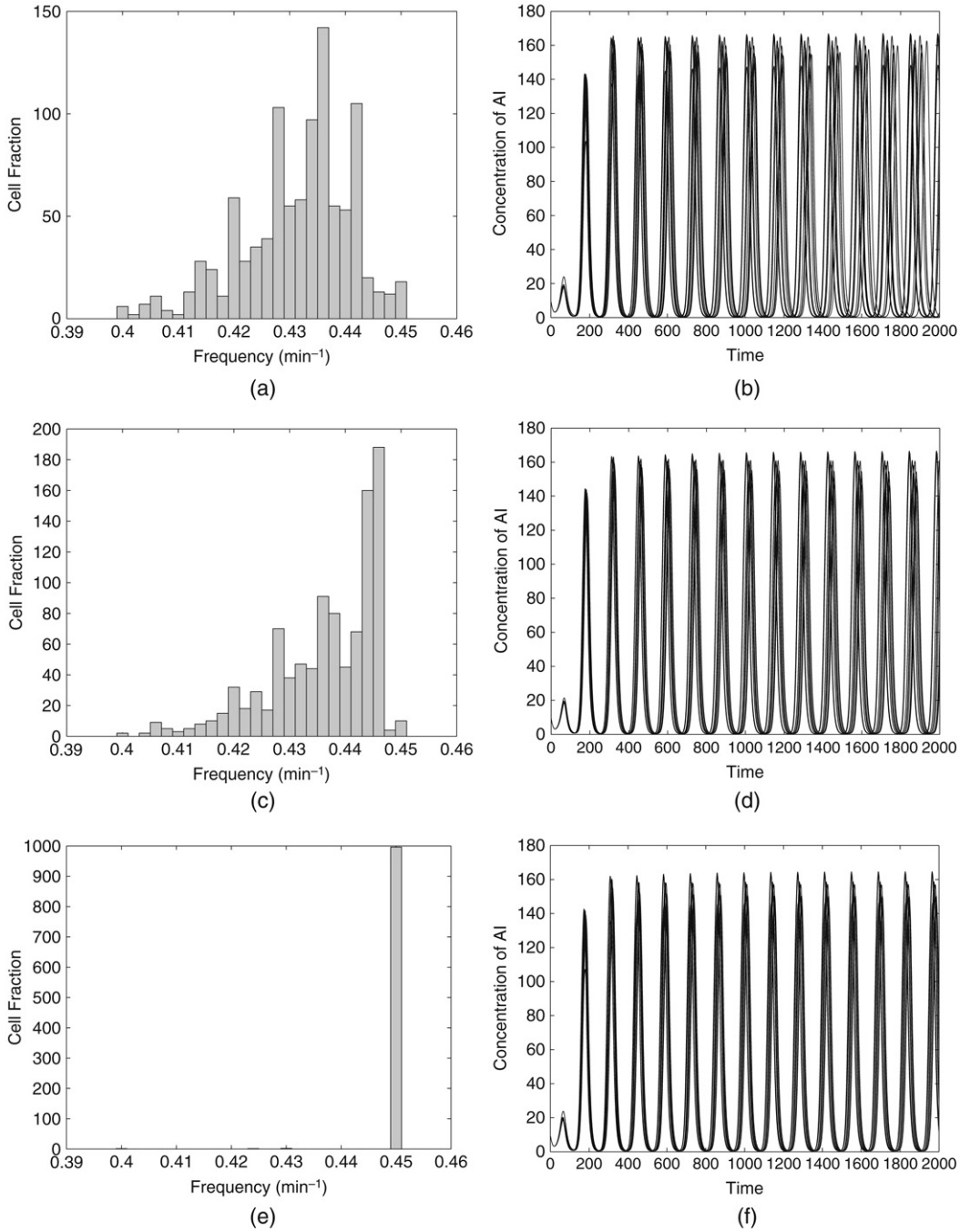


Fig. 3.3. Frequency histograms and time series plots for (a) & (b) $Q = 0.2$, (c) & (d) $Q = 0.4$ and (e) & (f) $Q = 0.6$, for the single tumour case when $N = 1000$.

and $k = 100$. We find that there is synchronization among the cells of all the tumours in the system upon strong coupling (see Fig. 3.6). The degree of synchronization increases with increase in the value of $Q$.

We also plot the power spectrum of certain cells in order to verify the presence of synchronization. For the local case, we take the data from 10 cells of a single tumour and superpose them (cf. Fig. 3.4(a)). Here too the first peak is found to coincide for all the cells. For the global case, we plot the data from 10 cells in different tumours. In this case, as well, we find the first peak coinciding, hence confirming the fact that the system is synchronized both locally and globally.

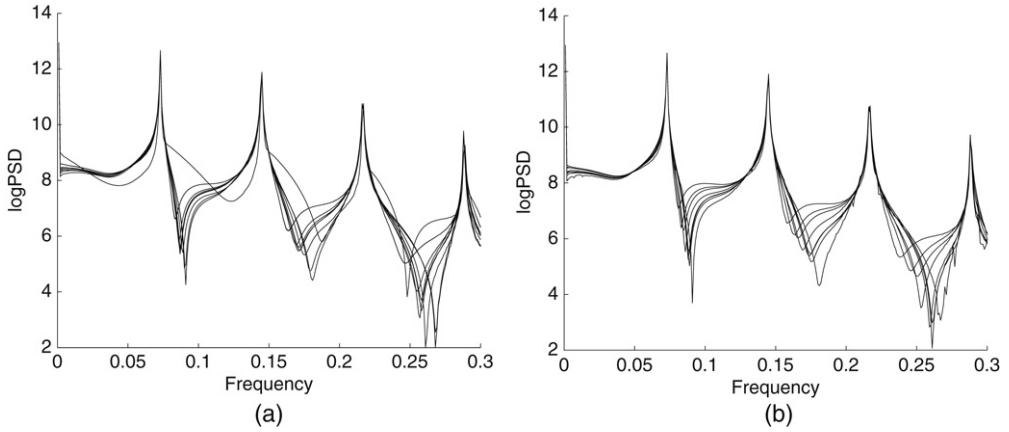


Fig. 3.4. Power Spectra of (a) 10 cells from one tumour and (b) 10 cells from different tumours, superimposed to demonstrate the local and global synchronization respectively.

## 4. Discussion

In our study of a system of coupled tumours, each individual tumour has a number of cells that oscillate independently. When the strength of coupling is small, there is a large spread of frequencies. This can be explained by considering the definition of our control parameter, $Q$, given by

$$Q = \frac{\delta N / V_{\text{ext}}}{k_{se} + \delta N / V_{\text{ext}}}.$$

This implies that when $\delta N / V_{\text{ext}}$ is small compared to $k_{se}$, $Q$ is also small. Since $k_{se}$ is a constant, this would mean a smaller value of $\delta N / V_{\text{ext}}$ which would indicate that the system consists of tumours present in relatively low concentration. As a result, there should be little or no synchronization among the cells. Our results indicate that this is, indeed, what happens.

The situation is qualitatively different when we increase the strength of coupling. The higher value of $Q$ indicates a higher cell density, or a higher concentration of tumours. Therefore, one can expect to observe a significant synchronization among the cells of the tumours. Once again our numerical results conform to our prediction. The cells of the tumour synchronize almost instantaneously after the onset of coupling. The same situation occurs when we have several tumours coupled together. Moreover, in addition to the local synchronization within each tumour, there is a global synchronization phenomenon.

Our results are in fair agreement with those reported by Garcia-Ojalvo et al. [3] who carried out a similar study for an ensemble of oscillators with sinusoidal waveforms and McMillen et al. [2] who considered a collection of coupled genetic relaxation oscillators. However, both of these works considered a homogeneous mixture of cells in a solution, analogous to bacterial or fungal populations in a laboratory culture. The cells were assumed to be physically separate from each other.

While this forms the basis of our study, we add an additional element that would make the system closer, at least in principle, to tumours found in various organisms. We have considered here collections of cells, which are capable of exchanging material between themselves by diffusion, in addition to being coupled via quorum sensing. In our opinion the combined effect of diffusion and quorum sensing produces a much stronger coupling association, as diffusion is inherently a damping force. Our predictions are supported by the numerical results presented here. There is synchronization among the cells not only within each tumour but also globally in a system of as many as 100 tumours. We also observe that there is a synchronization of frequency and phase. The amplitudes of individual cells are often different, although quite similar in order of magnitude.

Our system includes the effect of noise through the incorporation of the fact that the lifetime ratio of each cell in the system is a randomly distributed variable governed by the Gaussian distribution having $\mu = 1$ and $\sigma = 0.05$. The variability introduced as a result of this adds to the relevance of our study. Indeed, we find also that when we increase the variability to larger proportions the synchronization is minimal, if at all. (The corresponding results are omitted for the sake of brevity.) The cells demonstrate a much larger spread of frequencies even for a significantly

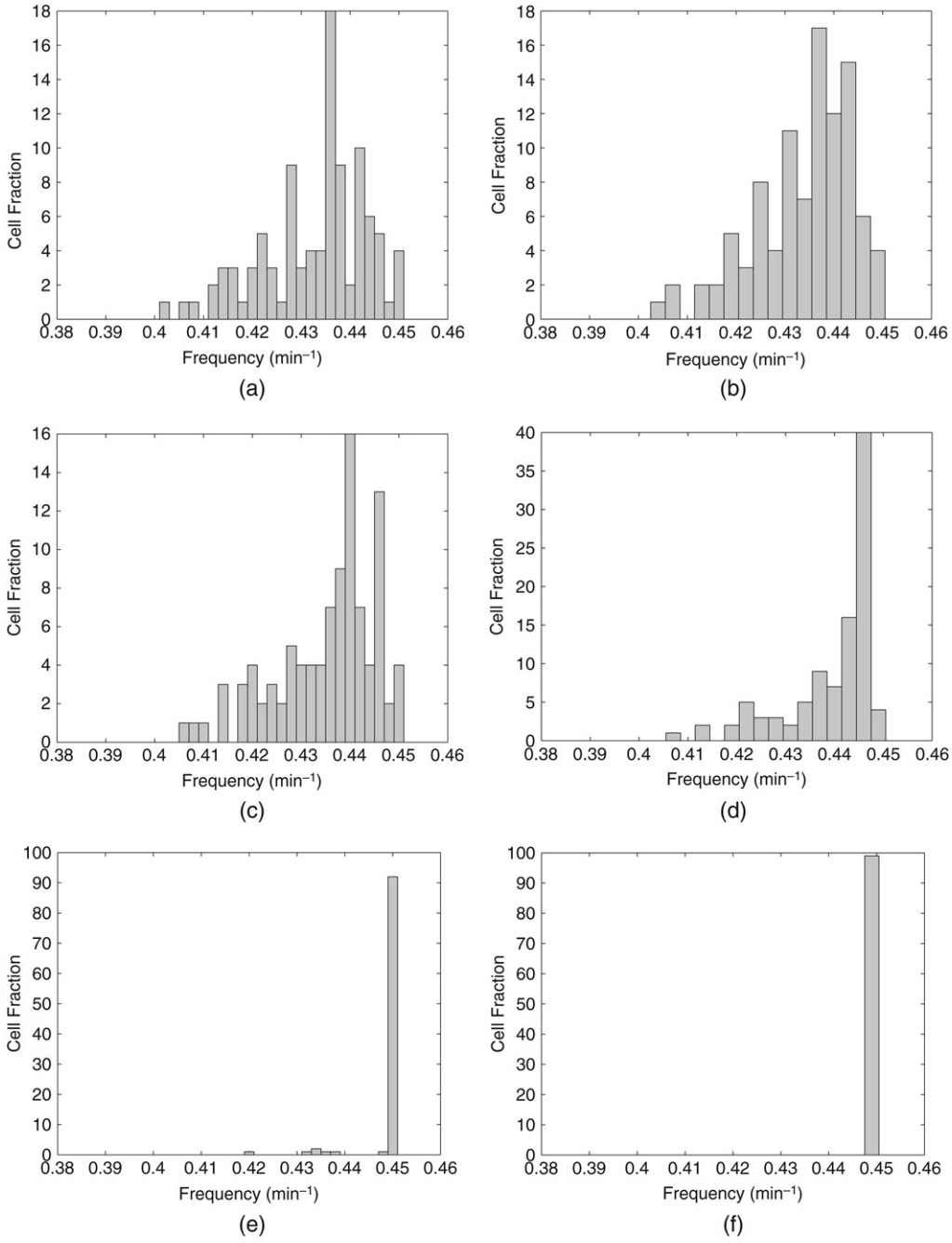


Fig. 3.5. Frequency histograms for one tumour when (a) & (b) $Q = 0.2$, (c) & (d) $Q = 0.4$ and (e) & (f) $Q = 0.6$, for the multiple tumour case with $N = 100$ and $k = 10$ (a), (c), (e) & $k = 100$ (b), (d), (f).

strong coupling factor. This indicates that the diffusion among neighbouring cells, although a strong damping force, is not strong enough to induce synchrony when there is much larger amount of noise in the system.

## 5. Summary and conclusion

In the preceding sections we have outlined the specific purpose of our study and subsequently examined, at length, the model that we have used. Numerical simulation of the model of the repressilator involved numerical integration of

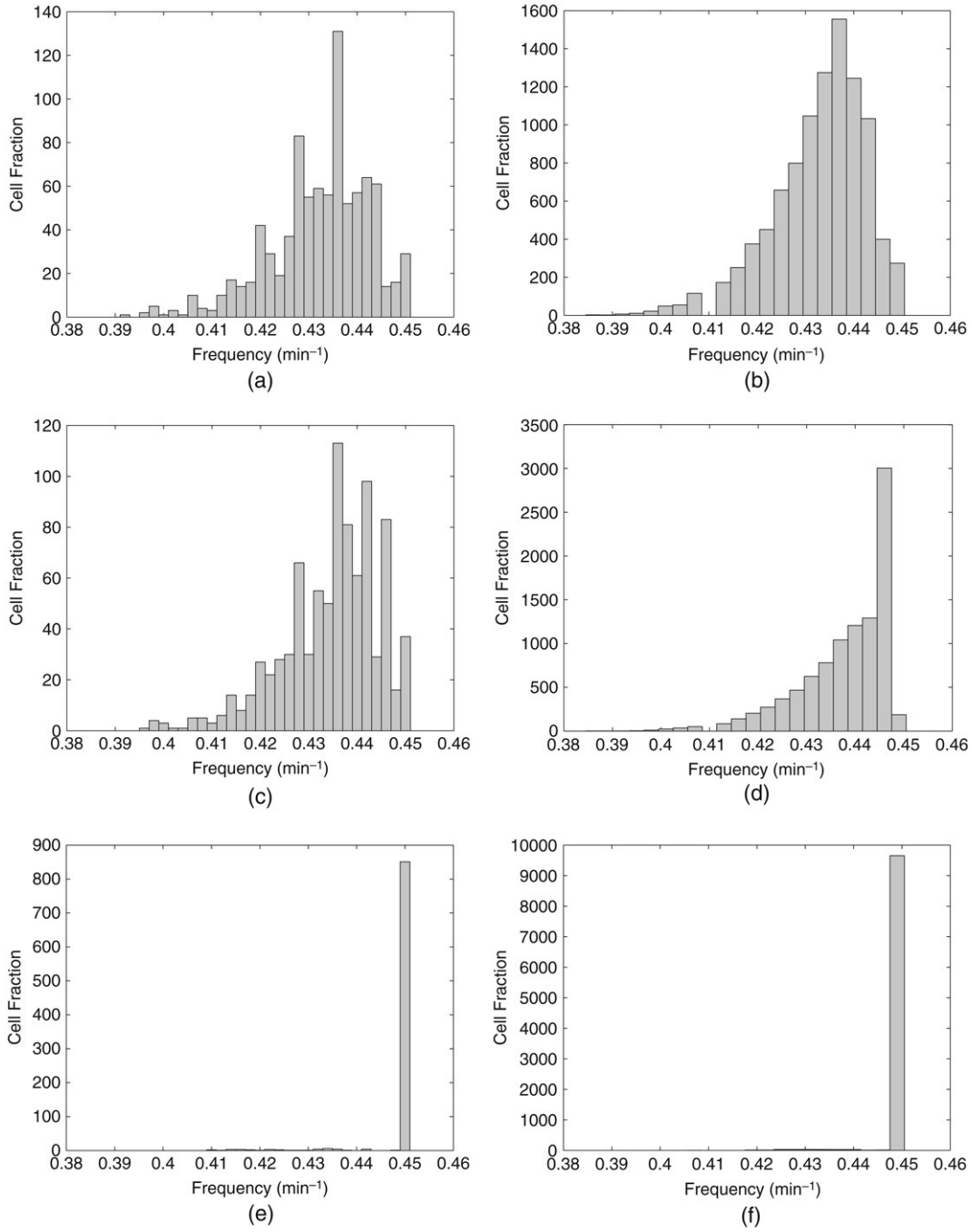


Fig. 3.6. Global Frequency histograms when (a & b) $Q = 0.2$, (c) & (d) $Q = 0.4$ and (e) & (f) $Q = 0.6$, for the multiple tumour case with $N = 100$ and $k = 10$ (a), (c), (e) & $k = 100$ (b), (d), (f).

the ordinary differential equations governing the system with the help of the Runge–Kutta fourth-order method. This problem is computationally demanding as it requires the solution of a coupled system of $N$ equations with the time required for the simulations increasing exponentially with increase in $N$. Moreover, we subsequently extended the system for one tumour, to a collection of tumours, hence increasing the computational demands of the program manifold.

The first part of the analysis involves a single tumour-like aggregation of cells. The external concentration of the auto-inducer (AI) molecule is rendered a constant as we adopt the quasi-steady-state approximation, which assumes

that the rate of change of the external concentration of AI is zero. In the case of the single cells in solution, the oscillations have been shown to synchronize in a robust manner, with the degree of synchronization determined by the strength of the coupling [3]. We have undertaken a generalization of this study by incorporating a diffusive mechanism between the neighbouring cells.

The second part of the analysis involves multiple cell aggregations. The quasi-steady approximation is still assumed to hold. We conduct the numerical simulations of the system with a view to verify whether there is the onset of synchronization in such a system as well. This is indeed found to be the case. Moreover, not only do the cells in each tumour synchronize amongst themselves, but there is also a global synchronization among all the cells in the system. This phenomenon is also found to depend on the strength of coupling.

In both the above cases we assume that the tumour-like growth is in a quiescent or non-proliferative state. A more general approach would be to consider the case where the tumours are growing. One could consider that the tumours are growing while in an avascular state, or at a latter stage of their development. There could be two ways of approaching this problem. One could numerically solve the partial differential equations involved in such a model and use it to determine the size of each tumour at each instant deterministically. However, that would involve solving the coupled system of both ordinary and partial differential equations that would be quite complex and in all probability, mathematically intractable.

Another property of the avascular tumour growth model indicates that the density of live cells drops drastically from the surface of the tumour to the interior. In other words, the only cells that are alive are present on or near the surface of the tumour. Hence, in this case, our assumption that only the cells on the surface of the tumour contribute to the external concentration of the AI molecule holds good. The only diffusion that occurs inside a tumour, takes place on its surface.

Therefore, a more feasible approach to the problem is to use the results of [4] to model the system. The tumours are predicted to grow at a linear rate after an initial nonlinear phase. The number of cells in each tumour would therefore become a linear function of time and we can deal with the resultant system with a lot more ease. The number of actively diffusing cells in each tumour, (which we have assumed to exist on its surface) would then become a linear function of its radius. Such a modification can therefore, be utilized and would provide us with a means of further extending our work in this direction.

The appearance of synchronization in a population of tumours is a remarkable finding. The clinical ramifications include possible clues towards a cure, as outlined in [8]. However, exciting as it may sound, this study can only be considered to be a stepping stone towards such an end. Indeed, we have used mathematical modelling of tumours in unison with genetic oscillators, for the purpose of demonstrating the characteristics that natural systems can exhibit.

Collections of oscillating cells having inherent differences can self-synchronize via various different ways, and quorum sensing is one of them. This mode of inter-cell signalling is an ancient way of communication developed and practiced by prokaryotic cells, such as bacteria and fungi. Aggregation of cells, such as tumours, is a eukaryotic phenomenon. It is quite possible that the cells of the sino-atrial node in mammalian hearts or the suprachiasmatic nuclei in the hypothalamus use different ways to synchronize their functions. However, the basic purpose of our study is to investigate the possibility that in the presence of a coupling factor among the cells, whether they would synchronize their functions in a local and global manner in order to remove noise from the system and increase their overall efficiency. Our findings indicate that this is indeed the case.

## References

[1] P. Hahnfeldt, D. Panigraphy, J. Folkmanm, L. Hlatky, Tumour development under angiogenic signaling: A dynamical theory of tumour growth, treatment response and postvascular dormancy, Cancer Res. 59 (1999) 4770–4775.

[2] D. McMillen, N. Kopell, J. Hasty, J.J. Collins, Synchronizing genetic relaxation oscillators by inter-cell signaling, Proc. Natl. Acad. Sci., USA 99 (2) (2002) 679–684.

[3] J. Garcia-Ojalvo, M.B. Elowitz, S. Strogatz, Modeling a Synthetic multi-cellular clock: Repressilators coupled by quorum sensing, Proc. Natl. Acad. Sci., USA 101 (30) (2004) 10955–10960.

[4] J.P. Ward, J.R. King, Mathematical modelling of avascular-tumour growth, Math. Med. Biol. 14 (1) (1997) 39–69.

[5] T. Roose, S.J. Chapman, P.K. Maini, Mathematical models of avascular tumour growth, SIAM Review 49 (2) (2007) 179–208.

[6] H.M. Byrne, T. Alarcon, M.R. Owen, S.D. Webb, P.K. Maini, Modelling aspects of cancer dynamics: A review, Phil. Trans. R. Soc. A 364 (2006) 1563–1578.

[7] A.R. Kansal, et al., Simulated brain tumor growth dynamics using a three-dimensional cellular automaton, J. Theoret. Biol. 203 (4) (2000) 367–382.
[8] N. Shitara, T. Kohno, K. Takakura, New approach to brain tumour chemoradiotherapy with cellular synchronization by colcemid, Acta Neurochir. 35 (1976) 123–133.